

Phase Transitions and the Nucleation of Catalytic Nanostructures under the Action of Chemical, Physical, and Mechanical Factors¹

S. A. Kukushkin and A. V. Osipov

Institute of Problems in Machine Science, Russian Academy of Sciences, St. Petersburg, 199178 Russia

e-mail: ksa@phase.ipme.ru

Received February 7, 2007

Abstract—Basic concepts of first-order phase transitions are formulated, and the state of the art in this field is considered using nanoparticle nucleation and growth as examples. General equations are presented to describe the nanoparticle size distribution function; the average nanoparticle radius; and the density, morphology, and composition of the new phase. Examples are given to illustrate the catalytic effect of nanoparticles on the kinetics of first-order phase transitions in multicomponent systems. The effect of the acidity (pH) of the medium on phase transitions in solutions and the effect of mechanical stress on the nucleation, evolution, and properties of quantum dots are considered.

DOI: 10.1134/S0023158408010102

The striking progress in microelectronics, optoelectronics, optics, and related fields of engineering in recent decades is due to the development of thin-film semiconductor technologies. In recent years, the focus of researchers' interest has shifted from continuous films to nanostructures. There is every reason to believe that the use of nanostructures in optics, microelectronics, chemistry, chemical catalysis, biology, and medicine will lead to a qualitative breakthrough in the technical development of mankind. Due to their developed surface, nanosystems possess unique properties. For example, nanocrystals usually have no dislocations or other linear defects. Furthermore, carrying out reactions on nanostructured catalysts may significantly change their rate and mechanism.

Nanostructures can be obtained by various methods. Nanocrystals on the surface of a solid substrate are obtained from the vapor, liquid, or solid phase. Various chemical and gas-transport deposition methods are very efficient. Among these, the sol–gel technology and electrodeposition are used to produce nanocrystals. Here, we will not consider particular methods of nanocrystal deposition on solid supports. Rather, we will focus on nanocrystal formation mechanisms.

Nanocrystal formation is a typical first-order phase transition. The size distribution of the resulting nanoparticles and, accordingly, the properties and the surface area and structure of the catalyst depend strongly on the way in which the phase transition takes place and on the transition rate. In this publication, we will touch upon the state of the art in nanocrystal production.

According to the classification dating back to Ehrenfest [1], all phase transitions can be divided into first- and second-order transitions. First-order phase transitions (PT I) are accompanied by abrupt changes of the first derivatives of the thermodynamic potential, such as entropy and density. Second-order phase transitions (PT II) are accompanied by abrupt changes in the second derivatives of the thermodynamic potential, such as heat capacity and compressibility. It is from the derivative orders that the phase transitions got their names. Formally, it is possible to introduce the concept of higher order phase transitions. For example, there are phase transitions of order 2.5 [2]; however, such transitions are rare and, for this reason, are not considered here.

THERMODYNAMICS OF PHASE TRANSITIONS

For a better understanding of the nature of phase transitions, we will refer to Landau's thermodynamic analysis of phase transitions [3]. To do this, we will consider such thermodynamic functions as free energy,

$$F(\eta) = U(\eta) - TS(\eta) \quad (1)$$

and the Gibbs potential,

$$\Phi = F(\eta) - pV. \quad (2)$$

In formulas (1) and (2), $U(\eta)$ is the internal energy of the system undergoing the phase transition, T is the temperature of the system, $S(\eta)$ is the entropy of the system, p is the pressure of the system, and V is the volume of the system. The parameter η is called the order parameter and characterizes the degree of order of the system. It ranges from zero for an entirely disordered

¹ Based on materials presented at the VII Russian Conf. on Mechanisms of Catalytic Reactions, St. Petersburg, July 2–8, 2006.

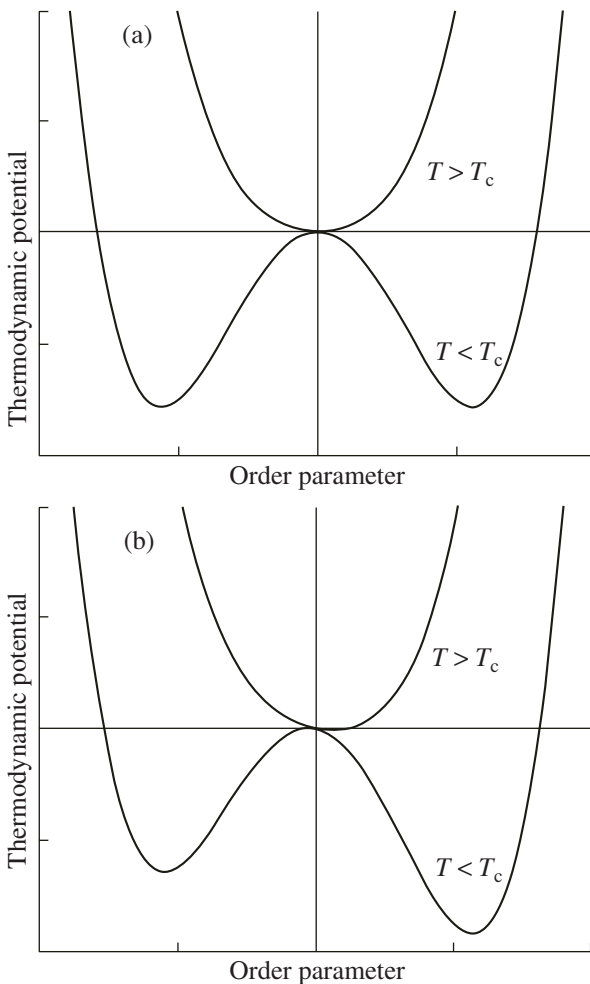


Fig. 1. Changes of the thermodynamic potential in (a) first- and (b) second-order phase transitions.

system to unity in an ordered system. The order parameter for different systems is defined as follows. For example, for solid solutions, $\eta = (\omega_A - \omega_B)/(\omega_A + \omega_B)$, where ω_A and ω_B are the probabilities of the atoms A and B being on some lattice site of the solid solution. For a liquid–vapor system, the order parameter is defined as $\eta = (\rho - \rho_{cr})/\rho_{cr}$, where ρ is the vapor density and ρ_{cr} is the vapor or liquid density at the critical point. For ferromagnets, the order parameter is the magnetization value: $\eta = M$. For ferroelectrics, the order parameter is vector polarization: $\eta = P$. According to Landau's theory, for PT II the Gibbs potential (2) near the transition point can be expanded into the following series in order parameter powers:

$$\begin{aligned} \Phi(p, T, \eta) &= \Phi_0(p, T) \\ &+ \alpha(p)(T - T_c)\eta^2 + B(p, T)\eta^4, \end{aligned} \quad (3)$$

where T_c is the second-order transition temperature or the Curie point and $\alpha(p)$ is the pressure-dependent component of the coefficient $A(p, T)$. Above and below the transition point ($T > T_c$ and $T < T_c$, respectively),

relationship (3) takes another form (Fig. 1a). It is clear from Fig. 1a that, in the case of PT II, the system passes from one state into another without having to surmount an energy barrier; that is, in the case of PT II, no metastable state of the matter is possible and all of the volume of the system changes its state. Now let us apply an external field to the system undergoing FT II, and let this system be below the Curie point. Equation (3) will then appear as

$$\begin{aligned} \Phi(p, T, \eta) &= \Phi_0(p, T) \\ &+ A(p, T)\eta^2 + B(p, T)\eta^4 - h\eta. \end{aligned} \quad (4)$$

It follows from Fig. 1b that the field changes the symmetry of the system. The positions of the minima and maxima of the Gibbs potential become inequivalent (Fig. 1b). The shallower minimum corresponds to the metastable state, and the deeper minimum corresponds to the stable state. To pass from one minimum to the other, the system has to surmount the potential peak $\Phi_{\max}(p, T)$. The field that causes this change in symmetry is the magnetic field ($h = H$) for ferromagnets and the electric field ($h = E$) for ferroelectrics. For gas–liquid transitions near the critical point, the analogue of the field is the quantity $h = p - bt$, where $p = P - P_{cr}$, P is pressure, P_{cr} is the pressure at the critical point, $t = T - T_{cr}$, T is temperature, T_{cr} is the temperature at the vapor–liquid transition critical point, and b is a coefficient in the expansion of the Gibbs potential in order parameter powers per unit volume (V) of the system: $b = B(p, T)/V$ [3]. Appreciable changes in symmetry take place in crystal formation and growth, vapor–liquid transitions, and the formation and growth of various films and nanostructures (i.e., in PT I). It is these phase transitions that will be considered below.

Thermodynamics of First-Order Phase Transitions

The principal difference between PT I and PT II is that, for the former, the Gibbs potential as a function of the order parameter at the transition temperature has two minima separated by an energy barrier. To pass from the metastable state to the stable state, the system has to surmount this energy barrier. As a consequence, the phase passes from one state to the other not throughout its volume, but in small portions, which are called nuclei of the new phase. The system has to form an interface, which requires a rather large amount of energy. The height of the barrier separating the stable and metastable states depends on the interfacial tension: the greater the interfacial tension, the less readily the system passes from one state to the other. For example, pure water freezes not at 0°C, but at a much lower temperature, because it is necessary to compensate for the energy consumption. According to classical nucleation theory, whose founders were Gibbs, Volmer, Weber, Becker, Döring, Frenkel, and Zel'dovich [4–8], the total change of the free energy upon the formation

of spherical particles of a new phase (nuclei) of radius R is written as

$$\Delta F(R) = -\frac{4}{3}\pi R^3 \Delta f + 4\pi R^2 \gamma, \quad (5)$$

where Δf is the difference between the free energies of the phases per unit volume of the system and γ is the interfacial tension. The first term in this equation accounts for the free energy change proportional to the nucleus volume. This term is negative because it is energetically favorable for the system to pass from the metastable state to the stable state. The second term is the free energy change proportional to the surface area. This term is positive because the formation of a surface requires an energy input. Figure 2 schematically shows the plot of Eq. (5). It can be seen from Fig. 2 that the new-phase nucleus whose radius corresponds to the maximum of function (5) is at unstable equilibrium. If the nucleus size is $R < R_{\text{cr}}$, the nucleus will dissolve since a decrease in its size will cause a decrease in the free energy ΔF . Conversely, a nucleus whose size is $R > R_{\text{cr}}$ will grow since an increase in R relative to R_{cr} will cause a decrease in ΔF . A nucleus of size R_{cr} is called a critical nucleus. If it has the shape of a sphere, its radius is calculated as

$$R_{\text{cr}} = \frac{2\gamma}{\Delta f}. \quad (6)$$

The work done on the formation of such a nucleus is

$$F(R_{\text{cr}}) = \frac{16\pi\gamma^3}{3(\Delta f)^2}. \quad (7)$$

As a system passes from one state to the other, numerous nuclei with $R < R_{\text{cr}}$ form there, and only very few of them pass from the $R < R_{\text{cr}}$ state to the $R > R_{\text{cr}}$ state. This transition takes place only by means of fluctuations and is, therefore, probabilistic in nature. As a consequence, the nuclei form not throughout the bulk of the old phase, but in separate regions in a random way. Some period of time is required for the new phase to fill the entire space of the old phase. The probability of the formation of a critical nucleus is calculated using the thermodynamic theory of fluctuations. The expression for this probability has the form of the conventional Boltzmann distribution function [3–8]:

$$W = e^{-F(R_{\text{cr}})/k_B T}, \quad (8)$$

where k_B is the Boltzmann constant and $F(R_{\text{cr}})$ is the work of the formation of a nucleus of the new phase (see Eq. (7)).

Let us generalize the above results for PT I in different systems. To do this, it is sufficient to write particular relationships for the free energy difference Δf . For a

gas–liquid system, $\Delta f \rightarrow \frac{k_B T}{\omega} \ln \frac{p}{p_0} \approx \frac{k_B T(p - p_0)}{\omega p_0}$;

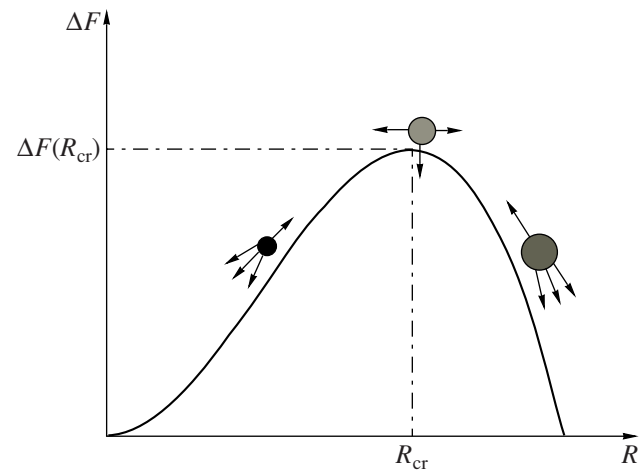


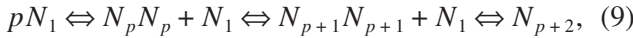
Fig. 2. Change of the free energy of formation of a spherical nucleus of a new phase in a first-order phase transition.

for solutions, $\Delta f \rightarrow \frac{k_B T}{\omega} \ln \frac{c}{c_0} \approx \frac{k_B T(\bar{c} - c_0)}{\omega c_0}$. Here, ω is the volume occupied by one atom (molecule) in a nucleus of the new phase; p and p_0 are the actual pressure in the system and the pressure corresponding to the equilibrium between the old and new phases, respectively; and \bar{c} , and c_0 are, respectively, the mean concentration of the substance in the solution and the equilibrium concentration [3–16]. For PT I in ferroelectrics (switching events) in an electric field below the Curie point, $\Delta f \rightarrow 2P_\infty E$. For ferromagnets with an easy magnetization plane, $\Delta f \rightarrow 2M_\infty H$. Here, P_∞ and M_∞ are the equilibrium values of polarization and magnetization [17].

KINETICS OF FIRST-ORDER PHASE TRANSITIONS

The main purpose of kinetic studies of phase transitions is to determine the number and size of the appearing nuclei of the new phase. Let us turn to formula (8), which describes the magnitude of the fluctuations of the number of nuclei. Usually, these are fluctuations of the density of atoms or molecules and are not directly related to nucleation. It turned out that, during phase transitions, so-called heterophase fluctuations take place along with density fluctuations. The existence of heterophase fluctuations was for the first time hypothesized by Frenkel [6]. He assumed that, along with the fluctuations of the density of atoms, there are fluctuations of subcritical nuclei, which are present in the old phase even when it is far from the transition point (line). It is these fluctuations that are responsible for the nucleation of the new phase. Earlier, the German physicist Volmer hypothesized that the nuclei of the new phase grow not via a sudden large fluctuation, but via the gradual addition of molecules of the old phase to the

nuclei of the new phase [5]. These fluctuations are similar to bimolecular reactions and can be represented as



where N_1 is the smallest heterophase fluctuation consisting of p atoms. This fluctuation is the precursor of a nucleus of the new phase. Once the number of atoms in a heterophase fluctuation or in a subcritical nucleus has reached the critical value, a further increase in the nucleus size will reduce the free energy ΔF and, accordingly, the nucleus will become stable. Calculating the number of these nuclei and predicting their future lives is the purpose of the kinetic theory of new-phase nucleation. The number of nuclei appearing in a unit time in a unit volume of the old phase is called the formation rate of the new phase or the nucleation rate. The mathematical expression for this flux is very similar to the formula describing the flux of diffusing atoms. This formal similarity is due to the fact that the atomic diffusion equation is a particular case of the more general equation called the Fokker–Planck equation. An analogue of the Fokker–Planck equation applicable to nucleation kinetics was set up by Zel'dovich [8]. The Zel'dovich equation appears as

$$\begin{aligned} \frac{\partial g(i, t)}{\partial t} &= -\frac{\partial}{\partial i} W_{i, i+1} \\ &\times \left[\frac{1}{k_B T} \frac{\partial \Delta F(i)}{\partial i} g(i, t) + \frac{\partial g(i, t)}{\partial i} \right], \end{aligned} \quad (10)$$

where $W_{i, i+1}$ is the diffusion coefficient of the nuclei of the new phase in the “size space,” which accounts for the probability of a nuclei passing from the size i to the size $i + 1$; $\Delta F(i)$ is the change of the free energy of the system, which depends on the number of structural units (i) in the nucleus of the new phase; $g(i, t)$ is the function of nucleus distribution over the number of structural units i at the time moment t ; and $N(t) = \int_0^\infty g(i, t) di$ is the total number of nuclei. The quantity i is understood here as the number of structural units of the old phase. The structural units in the water–ice and vapor–water transitions are water molecules, the structural units in copper crystallization are copper atoms, the structural units in switching events in ferroelectrics are whole unit cells corresponding to a certain direction of the polarization vector, and so on. For a spherical nucleus, the number of structural units is related to its radius by the simple expression $i = \left(\frac{4\pi R^3}{3\omega} \right)^{1/3}$, where ω is the volume per structural unit in the nucleus of the new phase.

The addition of molecules to the surface of a nucleus increases the nucleus size, and the abstraction of molecules from the nucleus diminishes it. These processes are random; as a consequence, the nucleus moves now to the right, now to the left, along the size axis (Fig. 2). This motion is irregular, like the motion of Brownian

particles in diffusion processes. This is reason why this motion is called diffusion in the “size space,” and the analogue of the diffusion coefficient here is the coefficient $W_{i, i+1}$. PT I events are accompanied by a change in the nucleus size distribution. The nuclei “flow” from the region in which their concentration is higher to the region in which their concentration is lower. The size distribution of these nuclei is described by the function $g(i, t)$. This function is an analogue of the atom concentration; however, as distinct from the latter, it defines the number of nuclei of given size in a unit volume of the old phase. The growth rate of a nucleus of the new phase (V_i) is given by the equation

$$V_i \equiv \frac{di}{dt} = -W_{i, i+1} \frac{1}{k_B T} \frac{\partial \Delta F}{\partial i}. \quad (11)$$

It follows from Eq. (11) that, to the left of the point of the maximum of the function ΔF (Fig. 2), where the nucleus size is subcritical, the growth rate is negative and the nuclei will dissolve. Conversely, supercritical nuclei will grow because their growth rate is positive. The growth rate of a critical nucleus is zero because $\frac{\partial \Delta F}{\partial i} = 0$ at the point of the maximum of the function (Fig. 2).

Thus, it follows from Eq. (10) that subcritical nuclei can grow only via the random addition of molecules of the old phase to their surface; that is, they diffuse in the “size space.” Since their regular growth rate is negative, the following procedure is used to derive particular forms of relationship (11) and to determine the coefficient $W_{i, i+1}$ [10, 11, 14–19]. Initially, the growth mechanism of the nucleus of the new phase is determined. For example, there are two basic mechanisms of the isothermal growth of nanostructures from one-component vapor on the surface of crystalline substrates. One is matter transport (i.e., diffusion) to an island, and the second is the transfer of atoms across the interface between the old and the new phases (boundary kinetics). Figure 3 schematizes the five basic mechanisms of nanostructure growth from one-component vapor. Mechanisms 3a and 3b describe the growth of unfaceted (left) and faceted (right) islands of the new phase on a smooth surface. The mechanism depicted in Fig. 3c describes the growth of islands on substrates having linear defects. In turn, each of these mechanisms can take place in two regimes: the growth rate can be controlled either by atomic diffusion or by boundary kinetics. It is clear from Fig. 3 that, in some cases, atoms from the vapor phase are initially adsorbed by the surface (Fig. 3a) and then diffuse toward the island and add to it along its perimeter. In other cases (Fig. 3b), atoms from the vapor phase are fixed directly on the island surface. In island growth on stepped surfaces (Fig. 3c), the atoms are initially localized on a smooth area of the substrate, and then they diffuse to the step to incorporate into the island. In the general case, the growth mechanism can be complicated. For

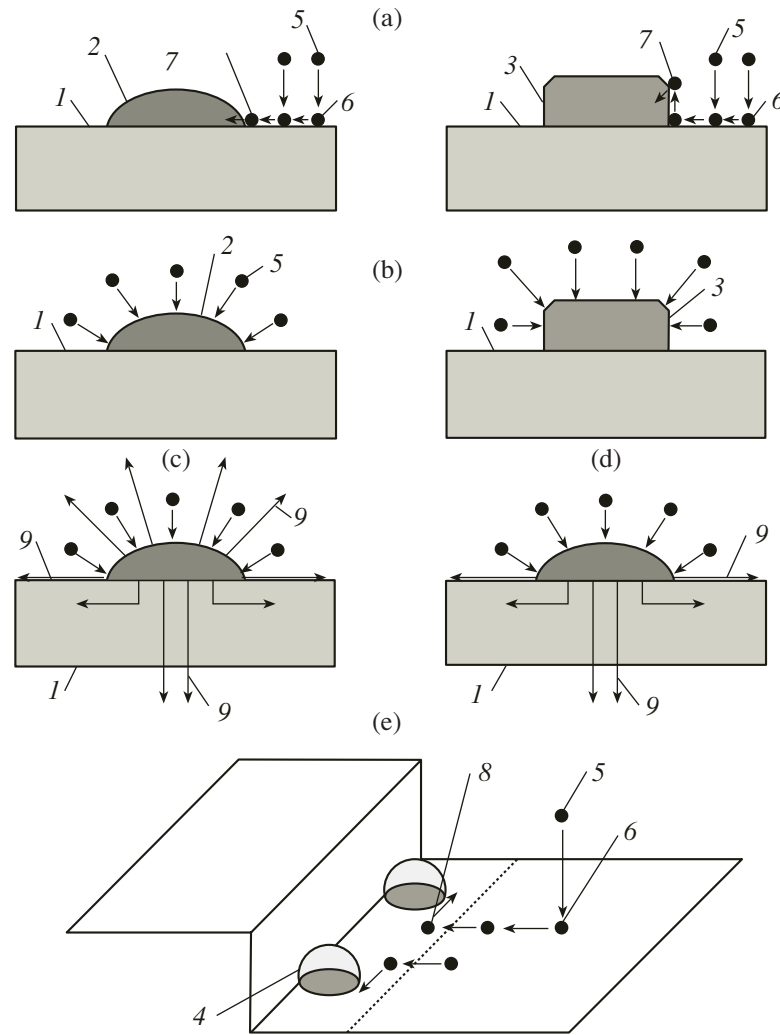


Fig. 3. Basic island growth mechanisms [15]: (a) growth of faceted and unfaceted islands controlled by the surface diffusion of the adatoms; (b) atomic diffusion in the vapor phase or evaporation/condensation; (c) growth of unfaceted islands via matter adsorption from the vapor phase onto their surface, with heat removed through the entire surface; (d) the same, but with heat removal only through the substrate; (e) island growth by linear diffusion along the steps of the substrate. (1) Substrate; (2) unfaceted island; (3) faceted island, whose surface adds atoms only in certain places; (4) island at a substrate step; (5–8) atom in the vapor phase, on the substrate surface, on the island surface, and at the substrate step, respectively; (9) heat fluxes.

example, in many cases, it is necessary to take into account the heat released and withdrawn during the growth of the islands. The islands may grow via chemical reactions, and this case will be considered below. In ferroelectric PT I events, the growth of the nuclei of the new phases is determined by the displacement of atoms in the unit cells from one equilibrium state to another [17]. It was proved theoretically [14–19] that all the mechanisms, irrespective of their nature, can be described by the following equation (in the quasi-steady-state approximation):

$$\frac{di}{dt} = m \frac{\xi(t)}{t_0} t^{(m-1)/m}, \quad (12)$$

where $\xi(t)$ is a dimensionless quantity characterizing the deviation of the system from the equilibrium state;

t_0 is a constant having dimensions of time, called the characteristic island growth time; and m is the growth index, which, for any system, takes only positive values ($m = 1, 3/2, 2, 3$) and depends on the shape of the island and the type of the rate-limiting step. The constant t_0 involves all the basic kinetic coefficients governing the island growth rate. Consider the quantity $\xi(t)$. For nanoparticle growth from solutions, $\xi(t) = \frac{c(t)}{c_\infty} - 1$ (supersaturation); for nanoparticle growth from the melt, $\xi(t) = 1 - \frac{T(t)}{T_\infty}$ (supercooling). For phase transitions in ferroelectrics, $\xi(t) = \frac{P(t)}{P_\infty} - 1$. This quantity was introduced in our earlier publication [17] and is called super-

polarization. In the expressions for $\xi(t)$, the quantities $c(t)$, $T(t)$, and $P(t)$ are the initial values of concentration, temperature, and polarization, respectively, and c_∞ , T_∞ , and P_∞ are the corresponding equilibrium values. Supersaturation, supercooling, superpolarization, and the like are the driving forces of phase transitions. As the particles grow in the course of a phase transition, they increasingly adsorb matter from the old phase and reduce $\xi(t)$. In turn, this slows down the growth of the nanoparticles and shifts the nucleation barrier (Fig. 2) to larger radii. Therefore, for determining the number of nanoparticles formed and the particle size distribution, it is necessary to supplement Eq. (10) with a $\xi(t)$ conservation equation. For nanoparticle growth on a solid substrate, the $\xi(t)$ conservation law appears as

$$\xi(t) = \xi_0 + \tau^{-1} \int_0^t [\xi_0 - \xi(t')] dt' + n_e^{-1} \int_0^\infty g(i, t) idi, \quad (13)$$

where ξ_0 is the initial supersaturation on the substrate $\xi_0 = J_0 \tau / n_e - 1$, J_0 is the flux of atoms being adsorbed from the medium onto the surface, τ is the lifetime of adsorbed atoms (called adatoms) on the surface, and n_e is the equilibrium concentration of adatoms. For phase transitions in the other systems, the universal law (13) will have the same form, but ξ_0 will take another particular form. For example, for growth from the melt,

$$\xi_0 - 1 - \frac{T^0}{T_\infty}, \text{ where } T^0 \text{ is the initial melt temperature.}$$

For ferroelectrics, $\xi_0 = \frac{\chi \varepsilon_0 E^0}{P_\infty}$, where χ is the relative dielectric susceptibility, ε_0 is the vacuum permittivity, and E^0 is the strength of the external electric field. The characteristic time should be modified in a similar way. For example, for phase transitions in ferroelectrics, $\tau = k_B T \chi \varepsilon_0 / 2 \beta_0 p_{zi}^2$, where β_0 is the kinetic coefficient describing the velocity with which atoms in crystal sublattices pass from one state into another.

Equations (10)–(13) provide a basis for the kinetic description of first-order phase transitions in any single-component system. They make up a complicated nonlinear set of equations. The problem of solving such equations is nontrivial, and many researchers continue developing mathematical approaches to this problem [9–11, 13, 15, 16, 18]. At present, the most promising approach is that in which characteristic stages of the phase transition are separated and characteristic times are introduced for each of them. “Rapid” and “slow” variables are introduced for the characteristic times. Solutions are sought for each stage and are then joined. Three characteristic periods of time are usually distinguished. In the first period, supersaturation is fairly high because the nuclei of the new phase are so few that they have been unable to absorb a sufficient number of atoms. Therefore, to determine the characteristics of

nucleation at this stage, it is sufficient to solve Eq. (10), while Eq. (13) may be left out of consideration and $\xi(t)$ can be taken to be constant. At this stage, nuclei form only by fluctuations. The solution of Eq. (10) for this stage is

$$I = n_1 \sqrt{-F''(i_{cr})/2\pi k_B T} W(i_{cr}) \exp(-F(i_{cr})/k_B T), \quad (14)$$

where $W(i_{cr})$, $F(i_{cr})$, and $F''(i_{cr})$ are, respectively, the diffusion coefficient in the “size space,” the work of formation of a critical nucleus, and the second derivative of the free energy at the critical nucleus size point and n_1 is the density of adatoms at the phase transition onset time. The calculation of $W(i_{cr})$ has already been discussed. For example, for the growth of new-phase nuclei on a substrate via the surface diffusion mechanism (Fig. 3), this coefficient is equal to

$$W(i_{cr}) = 2\pi R_{cr} n_1 l_0 (v_d/4) \exp(-E_d/k_B T) = 2\pi R_{cr} n_1 D_a / l_0, \quad (15)$$

where $D_a = (l_0^2 v_d/4) \exp(-E_d/k_B T)$ is the diffusion coefficient of adatoms on the substrate for disc-shaped two-dimensional particles, R_{cr} is the radius of the critical nucleus, E_d is the activation energy of surface diffusion, and l_0 is the diffusion hop length (which is of the same order of magnitude as the lattice constant of the substrate). Expression (14) is Zel'dovich's famous solution. It is applicable only to the earliest stages of nucleation.

In reality, extensive nucleation takes place rather rapidly. Sometimes, most of the substance transforms into a new phase within a few tens of microseconds. In this case, supersaturation cannot be considered to be constant. In the analysis of such a process, the set of equations (10)–(13) is considered not throughout the range of island radius values (Fig. 2), but only near the maximum of function (7), that is, near the critical radius of the new-phase nucleus. This makes it possible to simplify Eqs. (10)–(13) and to use the value of flux (14) as a boundary condition. As a result, the set of equations is solvable by the perturbation method applied to the small parameter $\epsilon = 1/\Gamma$ ($\Gamma = i_{cr} \gg 1$, where i_{cr} is the number of particles in the critical nucleus at $\xi = \xi_0$). The solution appears as

$$\xi(t) = \frac{\xi_0}{1 + (1/\Gamma) T^k(t) \varphi_k(T(t))}, \quad (16)$$

$$I(t) = I(\xi_0) \frac{\exp[-T^k(t) \varphi_k(T(t))]}{1 + (1/\Gamma) T^k(t) \varphi_k(T(t))}, \quad (17)$$

$$N(t) = I(\xi_0) t_k \varphi_k(T(t)), \quad (18)$$

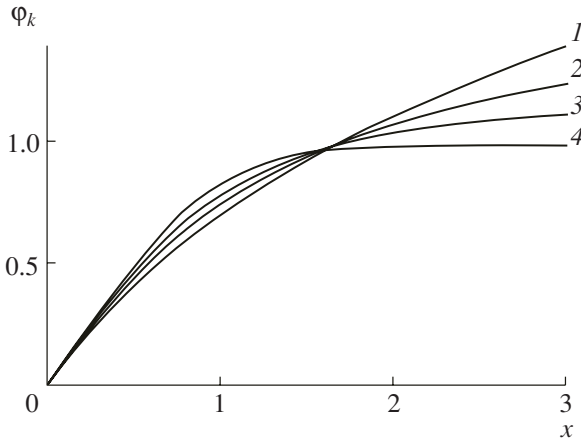


Fig. 4. ϕ_k as a function of x ; $k = (1) 0, (2) 1/2, (3) 1$, and (4) 2.

$$g(\rho, t) = \begin{cases} \frac{I(\xi_0)t_0}{\xi_0} \exp \left[-\left(T(t) - \frac{t_0 \rho}{t_k \xi_0} \right)^k \right] \\ \times \phi_k \left(T(t) - \frac{t_0 \rho}{t_k \xi_0} \right), & \rho \leq \xi_0 \frac{t_k}{t_0} T(t) \\ 0, & \rho > \xi_0 \frac{t_k}{t_0} T(t), \end{cases} \quad (19)$$

$$T(t) = \frac{t}{t_k} - \frac{1}{\Gamma} \int_0^t x^k \phi_k(x) dx, \quad (20)$$

$$t_k = \frac{t_0}{\xi_0} \left[\frac{n_e \xi_0}{(k+1) \Gamma I(\xi_0) \tau} \right]^{\frac{1}{k+1}}.$$

In Eqs. (16)–(20), the coefficient k is determined by the nanoparticle growth mechanism, which is related to the coefficient m in Eq. (12) as $k = m - 1$; $\rho = t^{1/m}$; $\xi(t)$ is supersaturation at the time t ; $N(t)$ is the density of nanoparticles at the time t ; $g(\rho, t)$ is the nanoparticle size (ρ) distribution function; $\phi_k(x)$ is an auxiliary function [15]; and $T(t)$ is renormalized time. Equations (16)–(20) describe the kinetics of PT I in all systems, irrespective of their physicochemical nature. The time dependences of the nucleation rate and of the new-phase island size distribution function are plotted in Figs. 4–6.

THE LATEST STAGE OF THE PHASE TRANSITIONS

During a phase transition, the number of particles on the substrate surface increases and the particles themselves grow. Due to this increase in nanoparticle density and size, the nanoparticles absorb increasing amounts of the substance from the surface. If the flux of atoms onto the substrate decreases with time, the supersaturation ξ on the surface tends to zero. Obviously,

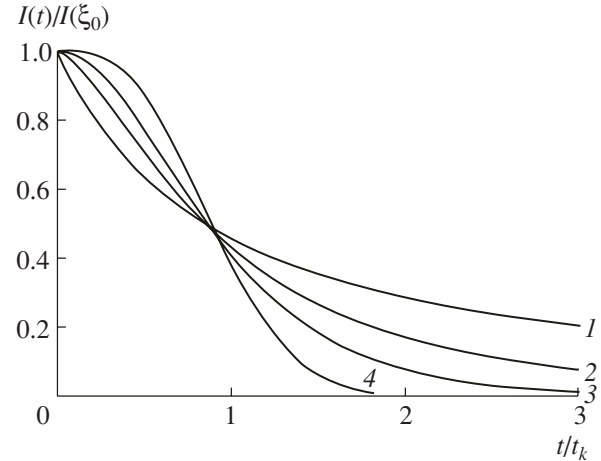


Fig. 5. Time variation of the nucleation rate at $\Gamma = 10$. $k = (1) 0, (2) 1/2, (3) 1$, and (4) 2.

new nanoparticles do not form under these conditions. The nanoparticles begin to interact in a specific way. This interaction takes place through the generalized self-consistent diffusion field of the adatoms. The islands of size $R < R_{cr}$ dissolve in the diffusion field because the equilibrium concentration of atoms, which depends on the island radius, is higher than the average concentration of atoms on the substrate. The islands of radius $R > R_{cr}$ grow because the equilibrium concentration of atoms there is lower than the average concentration of atoms on the surface. A specific feature of the behavior of the nanoparticle ensemble at this stage is that, as the supersaturation decreases, the critical radius R_{cr} increases, as follows from formula (6). If at some point in time the nanoparticle radius is larger than the critical radius and the nanoparticles grow, then it is possible that next moment their radius will be below the critical radius and they will dissolve. The nanoparticles whose radius is still above-critical absorb matter from

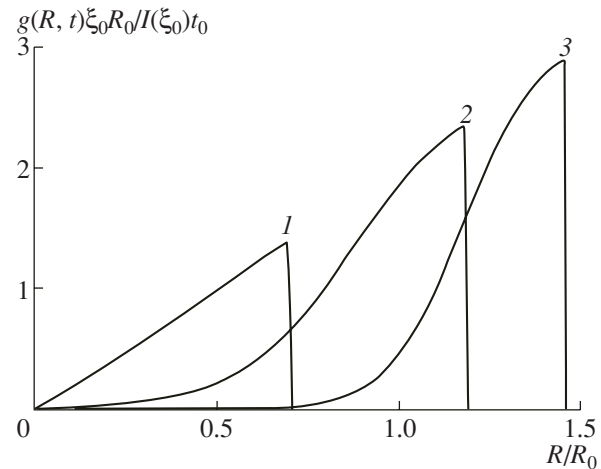


Fig. 6. Size distribution function for the islands of the new phase: $\Gamma = 10$; $k = 2$; $t = (1) 0.54t_k, (2) 1.7t_k$, and (3) $4.4t_k$.

the surface and thereby increase the critical radius in the system. However, it is possible that their radius will soon become subcritical and they will start to dissolve. In the infinite-time limit, a single particle would be expected to remain on the substrate surface. However, this will never happen, because, as the number of particles on the surface decreases, the interparticle distance increases. At some point in time, the free path length for the adatoms will become shorter than the mean interparticle distance and the generalized diffusion field will vanish. The adatoms that are far from the particles will evaporate from the surface before they can add to a particle. In real systems, the density of islands is fairly high and adatoms are continuously supplied to the surface. On reaching some size, the islands collide with each other and the process stops. This last stage of the phase transition is called Ostwald ripening. The mathematical analysis of this process, like the analysis of the previous stage, is based on Eqs. (10)–(13). For the first time, Eqs. (10)–(13) for the evolution of the new phase at the Ostwald ripening stage were solved by Lifshits and Slezov [20]. In a later monograph [21], we obtained a rigorous asymptotic solution describing the evolution of an ensemble of new-phase nuclei at the Ostwald ripening stage. This solution is somewhat different from Lifshits and Slezov's solution. The solutions presented in [20, 21] prove that any arbitrarily complex system consisting of an ensemble of new-phase nuclei in the old phase is governed by the following universal law at the latest stage of the phase transition:

$$R_{\text{cr}}(t) = \text{const} t^{1/p}, \quad (21)$$

$$N(t) = \text{const} t^{n-d/p}, \quad (22)$$

$$f(R, t) = \frac{N(t)}{R_{\text{cr}}(t)} P_p^s \left(\frac{R}{R_{\text{cr}}(t)} \right), \quad (23)$$

$$P_p(u) = \frac{u^p}{u^{p+1} - (p+1)u + p} \times \exp \left[\frac{d-n(p+1)}{2} \int_u^{u_p} \frac{x^p dx}{x^{p+1} - (p+1)x + p} \right], \quad (24)$$

where $P_p(u)$ is the distribution function normalized to unity so that $\int_0^\infty P_p(u) du = 1$,

$$v_p(u) = \frac{p^p (p-1)^{-(p-1)} (u-1) - u^p}{p u^{p-1}}, \quad (25)$$

and $u = (p-1)R/pR_{\text{cr}}$. Here, $P_p(u)$ is the particle size distribution function for the new phase at the time t ; $N(t)$ is the density of nuclei of the new phase; $\bar{R}(t)$ is the average nucleus radius; p is a coefficient depending on the nucleus growth mechanism, which is related to the above-introduced coefficient m as $p = d/m + 1$, where $d = 2$ or 3 , depending on the dimensionality of

the space in which the phase transition occurs (for nuclei on a substrate surface, $d = 2$; for nucleus growth in a three-dimensional system, $d = 3$). $P_p(u)$ is a unified function. Its particular forms for different new-phase growth mechanisms can be found, e.g., in [14, 16, 19–21]. The argument of this function is $u = (p-1)R/pR_{\text{cr}}$.

One of the most important theoretical results is that a universal nucleus size distribution independent of the initial conditions forms at the latest stage of PT I. The distribution function retains its original form until the system comes to equilibrium. Thus, in the course of a phase transition, any system "forgets" its initial state and passes to the stable asymptotic state that is the same for all systems. This state is characterized by a universal distribution function $P_p(u)$ depending only on the growth mechanism of the new phase in the system.

CHEMISTRY AND PHASE TRANSITIONS

Here, we will demonstrate how phase transitions are affected by chemical factors, such as the presence of several components, the rate of the reactions taking place, and the acidity of the medium. These problems were addressed and discussed in detail in a number of earlier works [9, 13–16, 19, 22–27]. In this publication, we will briefly report the main results. Note that, no matter what the system, the number of components, etc., the above general approach to the analysis of phase transitions will be the same. All basic equations in their formal notation will also be the same.

Multicomponent Nanosystems

Multicomponent systems whose components are completely miscible in different phases. For phase transitions in such systems, the Zel'dovich equation appears in modified form. It is multidimensional, and the diffusion coefficient in the "size space" depends on the component concentrations in the system. The nucleation rate I (Eq. (14)) takes the form of

$$I = n_1 \left(\sum_{k=1}^m W_k \right) \exp(-H_0), \quad (26)$$

where W_k is the diffusion coefficient of the k th component of the m -component system in the size space at $i = i_{\text{cr}}$ [14, 15], H_0 is the barrier to multicomponent nucleation, and n_1 is the density of molecules in the initial phase. Particular forms of the expression for nucleus flux (Eq. (26)) for various systems can be found elsewhere [14–16, 22–24].

Catalyst effects on phase transitions. If, in a system undergoing a phase transition, complicated chemical reactions occur and yield a new phase catalyzing one of the intermediate reactions, then self-organization and autooscillations will be possible under certain conditions [14–16, 26]. Suppose that the substrate surface contains atoms of the substances A and B and that

their concentration is below the concentration necessary for the formation of nuclei from these components. Suppose that these components react to yield the product C . In the case of a large excess of the component B on the surface, the reaction rate will be controlled only by the concentration of the component A . Suppose now that the reaction product C catalyzes one of the intermediate steps of the reaction; that is, this substance initiates its own formation. Let the surface concentration of C exceed the equilibrium concentration C_∞ at some moment in time. The nuclei of a new phase from the product C will then begin, and the resulting nuclei will absorb atoms of the substances A and B . If the number of nuclei becomes sufficiently large, it will be possible that the number of the atoms A and B would be insufficient for the reaction to proceed and the concentration of the substance C on the substrate surface would be insufficient for the growth of the nuclei. When the concentration of C becomes lower than the equilibrium concentration, the nuclei will begin to dissolve. This will indicate that a negative feedback has appeared in the system: a decrease in the number of nuclei will cause their growth, and vice versa, a buildup of nuclei will cause their dissolution.

The substance C formation rate may depend not only on the reaction rate constant, but also on the diffusion rates of the atoms of A and B to the locus of the reaction. If this is the case, both time and space variations of the number of new-phase nuclei will be possible. According to Prigogine's definition, this process is called self-organization. However, the above circumstances are insufficient for self-organization to take place. It is necessary that the rate of substance C formation, which is assumed to be catalyzed by C itself, should be a nonlinear function of the concentration. The simplest nonlinearity has the form of kAC^2 , where k is the rate constant of the reaction. If these conditions are satisfied, time oscillations of the number of islands or spatial self-organization can occur in the system. For example, the time oscillations of the number of nuclei are described by the following set of equations:

$$\begin{cases} \frac{dA}{dt} = J_0 - kAC^2 \\ \frac{dC}{dt} = kAC^2 - \gamma NC \\ \frac{dN}{dt} = \beta_0(C - C_\infty). \end{cases} \quad (27)$$

In these equations, J_0 is the rate of the arrival of the component A at the surface, k is the rate constant of the chemical reaction, β_0 is the coefficient of proportionality between the concentration and growth rate of the islands of the new phase, and γ is another coefficient of proportionality.

Let us consider each of the three equations in (27). The first equation describes the rate of change of the component A concentration. This rate depends on the

flux J_0 and on the rates of component A conversion (kAC^2). The term kAC^2 means that the substance A itself reacts with the product C and thus activates its formation. The second equation indicates that the concentration of the product C increases owing to its synthesis in the reaction involving the component A and decreases because of the absorption of C by the islands of the new phase. The third equation in (27) describes the rate of increase of the number of nuclei. In the model considered, this rate is assumed to be proportional to the supersaturation value ($C - C_\infty$). An analysis of this set of equations [14–16, 26] demonstrated that, at a substance flux of $J_0 > kC_e^3 - \beta\gamma/k$, the behavior of the system may be unstable and sustained oscillations of the concentrations $N(t)$, $C(t)$, and $A(t)$ may occur there. The number of nuclei in such a system may fall to zero. Experimental studies of the growth of films of the high-temperature superconductor $\text{YBa}_2\text{Cu}_3\text{O}_{7-x}$ [28] gave a surprising result: at the earliest stages of growth, the density of islands oscillates. We studied a more general case of self-organization during phase transitions [14–16, 26]. It was demonstrated that self-organization takes place when the diffusion coefficient of the product (D_C) is far below the diffusion coefficient of the reactant A (D_A): $D_C \ll D_A$. Self-organization in this case takes place as follows. The nuclei of the new phase absorb the substance A from the surface and thus decrease its concentration. This slows down the reaction yielding the substance C . This reduces the driving force of nucleation. The diffusion of the components A and C causes spatial nonuniformity of their distribution over the surface and, accordingly, nonuniformity of the rate of nucleation on the substrate. Thus, the initial symmetry of the substrate changes and the entire system becomes spatially nonuniform. As a consequence, the film structure will vary over the substrate surface. For example, if the nuclei of the new phase are semiconductors having different band gaps, a system of heterostructures may appear on the substrate surface. The band gap in such a heterostructure will vary periodically over the substrate surface.

Effect of the acidity of the medium (pH) on the kinetics of first-order phase transitions and nanostructure formation. One method of heterostructure preparation is matter deposition from ionic solutions. In this method, the acidity of the solution, which is characterized by pH, may play a crucial role in the nanostructure nucleation kinetics. pH has a particularly strong effect on the size distribution function, composition, and structure of the resulting nanoparticles. By varying pH, it is possible to efficiently control these parameters and to obtain nanoparticle ensembles with desired properties. pH exerts its effect on the nucleation of the new phase by modifying the equilibrium concentrations of the components from which the nanoparticles grow. This changes the supersaturation value and, accordingly, all the basic parameters of the phase transition, including the nucleation rate and the nanoparti-

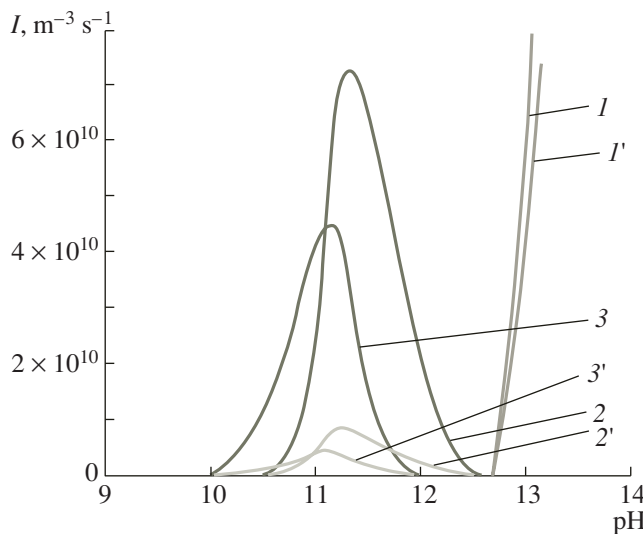


Fig. 7. pH dependence of the nucleation rate for aqueous solutions of $\text{Pb}(\text{OH})_2$ and CaCO_3 in the cases of diffusion-controlled nucleation ((1) $I_D(\text{Ca}(\text{OH})_2)$, (2) $I_D\text{Pb}(\text{OH})_2$, (3) $I_D\text{CaCO}_3$) and boundary kinetics-controlled nucleation ((I') $I_{SK}\text{Ca}(\text{OH})_2$, (2') $I_{SK}\text{Pb}(\text{OH})_2$, (3') $I_{SK}\text{CaCO}_3$).

cle size distribution function. The effect of pH on the nucleation rate was studied for the deposition of ionic salts from solutions [25]. In the case of nanoparticle growth controlled by boundary kinetics, specifically, the addition of atoms to the nucleus surface, the nucleation rate as a function of pH is expressed as

$$I_{SK}(\text{pH}) = n_1 \frac{\beta \sqrt{\gamma}}{2\pi \sqrt{k_B T}} \exp\left(-\frac{16\pi\gamma^3 \omega^2}{3\xi^2(\text{pH})(k_B T)^3}\right), \quad (28)$$

where β is the specific boundary flux (which depends on the abstraction/addition energy of atoms from/to the nucleus surface), n_1 is the density of molecules in the initial phase, and ω is the volume per molecule in the crystalline phase. The pH dependence of the supersaturation value for various ionic equilibria is reported in [25]. For crystallization of a poorly soluble base, such as $\text{M}^{n+} + n\text{OH}^- \rightleftharpoons \text{M}(\text{OH})_n \downarrow$, where M^{n+} is the ion of an n -valent metal and OH is the hydroxyl group, $\xi(\text{pH}) = \frac{K_w^n \exp((2.3\text{pH}n)C_+ - SP_{\text{M}(\text{OH})_n})}{SP_{\text{M}(\text{OH})_n}}$, where $SP_{\text{M}(\text{OH})_n} =$

$C_\infty^{n-} C_\infty^+$ is the solubility product, $K_w^n = 10^{-14}$ is the ionic product of water, C_∞^+ is the equilibrium concentration of metal ions, C_∞^- is the equilibrium concentration of hydroxyl groups, and C_+ is the concentration of metal ions at the onset of crystallization. Figure 7 plots the pH dependence of the nucleation rate for the crystallization of some poorly soluble salts and bases from aqueous

solutions in the cases of the crystal nucleation rate controlled by diffusion and boundary kinetics.

THE LATEST STAGE OF PHASE TRANSITIONS IN MULTICOMPONENT SYSTEMS

The Ostwald ripening processes in multicomponent systems are much more diversified than those in one-component systems because matter redistribution among nanoparticles is due not only to the difference in particle size, but also to chemical differences. A detailed analysis of this phenomenon can be found in [14–16, 19, 29]. The results obtained amount to the following. The general form of the nanoparticle ensemble evolution equations (Eqs. (21)–(25)) remains unchanged. However, now we have not one, but several sets of equations describing the evolution of each chemical compound (phase s). The number of these sets of equations is equal to the number of compounds constituting the nanoparticles. Equations (21)–(25) are supplemented by extra equations interrelating the common components of the phases and defining the phase coexistence regions (phase boundaries) during the evolution of the phases. The form of these extra equations depends on the initial concentrations of the substances, on their external sources, and on the heats of the chemical reactions occurring in the system.

FORMATION AND EVOLUTION OF NANOSTRUCTURES UNDER THE ACTION OF MECHANICAL STRESS

Films with a perfect crystal structure (so-called epitaxial films) can be grown if the lattice constants of the film and the substrate differ by no more than 7% [14, 15, 30–37]. At the initial stages of film growth, when nanoislands form, it is possible to obtain islands coherently conjugated with the substrate if the lattice mismatch is no greater than 7%. The formation of coherent islands (free of lattice mismatch-induced defects) during heteroepitaxial film growth was observed for the first time in 1990 [30] in the $\text{Ge}/\text{Si}(100)$ system with a mismatch value of 4.2%. Thus, a novel, dislocation-free film growth mechanism was discovered. Before 1990, it was believed that three-dimensional heteroepitaxial growth (so-called Stranski–Krastanov growth) can take place only as a result of the formation of lattice mismatch dislocations at the island/wetting layer boundary. Since then, interest in coherent nanoislands has been growing steadily [31–35]. In earlier works [36, 37], we suggested a theory of coherent Ge island growth on the $\text{Si}(100)$ crystal surface and reported a series of experiments fully confirming this theory. This coherent nanoisland growth theory [36, 37] is based on the above-described general principles of PT I theory and uses slightly modified Eqs. (16)–(20) to calculate the basic properties of the ensemble of coherent nanoparticles. There are two nanoisland growth mechanisms. The first is the classical Stranski–Krastanov

mechanism, which usually takes place in the case of a large lattice mismatch between the film and the substrate. According to this mechanism, the islands are not coherently conjugated with the substrate and mismatch dislocations appear as a result. The second mechanism is the modified Stranski–Krastanov mechanism. In the first mechanism, islands grow owing to the diffusion of adatoms on the substrate (Fig. 3). In the second, the strong interaction between the substrate and the material being deposited yields a thin (~3-nm) wetting layer on the surface. Since the deposited material is coherently conjugated with the substrate owing to the small lattice mismatch, the wetting layer has no dislocations and, as a consequence, is heavily strained. Increasing amounts of new atoms incorporate into the surface of this layer during the growth process. On the one hand, this increases the elastic stress energy of the wetting layer. On the other hand, this weakens the bonding between the substrate surface and the uppermost, newly formed layers of the material. At a certain thickness of this layer (let it be h_{eq}), the system comes to equilibrium. If the wetting layer thickness h is larger than h_{eq} , the layer is unstable and the nucleation of nanoparticles coherently conjugated with its surface is favorable. This growth mechanism is called island growth. If $h < h_{\text{eq}}$, the layer continues to grow and no nanoparticles form. This mechanism is called layer-by-layer growth. Thus, the h_{eq} value determines the crossover from 2D growth to 3D growth. The nanoparticles nucleating by this mechanism (their size does not usually exceed 100 nm) have no mismatch dislocations and, as a consequence, possess special physical properties. In physics, crystalline nanoparticles of semiconductors are called quantum dots because they have special energetic zones that are due to their small size and the absence of dislocations.

Let us introduce the quantity $\xi = \frac{h}{h_{\text{eq}}} - 1$. It will be

a measure of the driving force of quantum dot growth. It is nothing more than an analogue of supersaturation in PT I and has received the name of superstress [36, 37]. The growth mechanism of these nanoparticles is based on atomic diffusion, and the driving force of this diffusion is the relaxation of excess elastic energy. The value of h_{eq} is defined as follows [36, 37]:

$$h_{\text{eq}} = h_0 k_0 \ln \frac{\Phi_{\infty}}{\lambda \varepsilon_0^2 h_0}, \quad (29)$$

where $\Phi_{\infty} = \sigma_s - \sigma_f - \sigma_{s-f}$, σ_s is the surface tension of the substrate, σ_f is the surface tension of the film, σ_{s-f} is the film/substrate interfacial tension, h_0 is the thickness of a monolayer of the substance being deposited, k_0 is the coefficient that accounts for the screening of the interaction between the substrate and the wetting layers (for silicon–germanium layers, this coefficient was estimated in [30]), λ is the elastic modulus, $\varepsilon_0 = (d_f - d_s)/d_s$ is the film–substrate mismatch parameter, d_s is the lat-

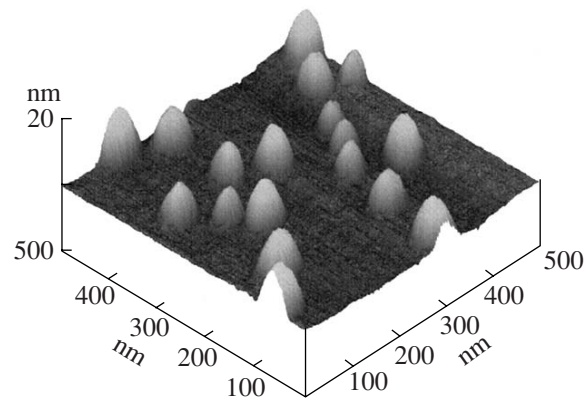


Fig. 8. AFM image of coherent islands (quantum dots) of Ge on the Si(100) surface at $T = 500^{\circ}\text{C}$ and an average deposition rate of 2 ML/min.

tice constant of the film, and d_s is the lattice constant of the substrate. Now that we have introduced ξ and h_{eq} , it is possible to calculate all the basic characteristics of quantum dot nucleation using Eqs. (16)–(20). This calculation was carried out in earlier works [36, 37], where all the basic characteristics of the evolution of quantum dots were determined. These are the nucleation rate and the size distribution, surface morphology, and density of the nanoparticles. By way of example, Fig. 8 presents an AFM image of Ge quantum dots on the Si(100) surface. These studies were continued in [38].

NANOPORE AND MICROCRACK FORMATION IN BRITTLE SOLIDS AND NANOFILMS

Of particular significance for the development of nanofilm technologies is the investigation of the formation and thermodynamic equilibria of microstructure defects (pores and dislocations) in the nanostructures and nanofilms forming on substrates at large lattice mismatches of 15–25%. The growth of such microstructures induces large mechanical stresses at the film/substrate interface. These stresses cause the nucleation of nanopores at the interface. Nanopore formation can significantly affect the properties of the catalyst being used. A theory of pore and microcrack formation in brittle solids was suggested in [39–41]. There are two main physical causes of microcracking [42]. These are the vacancy-induced nucleation of microcracks and the formation of microcracks due to dislocation coalescence. We have considered only the vacancy-induced nucleation of pores and microcracks. It was demonstrated that pore nucleation is similar to crystal nucleation from supersaturated solid solutions. There is always some equilibrium concentration of vacancies in the solid bulk. The vacancies in a solid, if their concentration is not high, are thermodynamically similar to an ordinary gas, which can condense into a liquid as the pressure is raised. For this reason, such a vacancy ensemble is called a vacancy gas [3, 6]. When a crystal

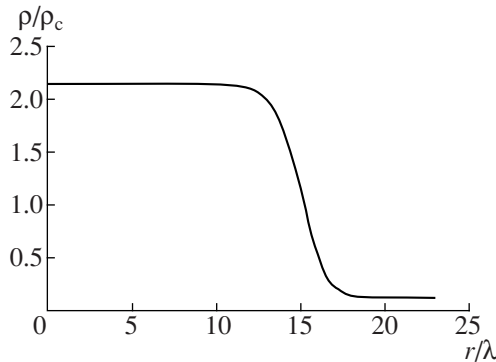


Fig. 9. Density profile for a liquid cluster in a van der Waals gas at $T = 0.7T_c$. T_c and ρ_c are the critical temperature and density of the gas, respectively; r is the distance from the cluster center; $\lambda = \sqrt[3]{\frac{m}{N\rho_c}}$; m is the mass of one molecule.

is extended, extra (overequilibrium) vacancies appear in it. This increases the density of vacancies, just as an increasing pressure raises the density of an ordinary gas. The vacancy buildup can cause pore nucleation. Thus, the vacancy gas and the pores can be treated as

two different phases. The quantity $\xi(t) = \frac{\sigma\omega}{k_B T} = \ln \frac{c_{v(t)}}{c_{v0}}$

(σ is the normal component of the stress tensor of the solid before the load is applied, ω is the volume of a vacancy, c_v is the vacancy concentration in the strained crystal, and c_{v0} is the equilibrium concentration of vacancies at a given temperature) is nothing more than an analogue of supersaturation. This parameter was introduced above and was called superstress [39, 40].

It was demonstrated that the pore nucleation rate under load is

$$I_0 = \frac{\gamma^{1/2} \beta_0 \sqrt{\delta}}{2\pi \sqrt{k_B T}} \exp\left[-\frac{16}{3} \frac{\pi \gamma^3 \delta}{k_B T \sigma^2}\right], \quad (30)$$

where β_0 is the equilibrium flux of the vacancies adding to the pore and leaving the pore, which is related to the vacancy diffusion coefficient, and δ is the change in the work of pore formation caused by the pore nonsphericity (usually, $\delta \approx 10^{-1}-10^{-2}$).

SURFACE TENSION AS A FUNCTION OF THE NANOPARTICLE SIZE

To conclude, we will note some structural features of the interface between a nanoparticle and the medium from which it forms. Earlier [43], we demonstrated that the structure of the nanoparticle/old phase interface is not sharp and has an intermediate region (Fig. 9). It was rigorously proved that the dependence of the surface tension on the nanoparticle radius in the principal order of perturbation theory is expressed as

$$\sigma(R) = \sigma_0 \frac{R + (d-1)\delta}{R} + O\left(\frac{1}{R^2}\right), \quad (31)$$

where R is the particle radius ($d = 3$ for drop-shaped particles, and $d = 2$ for disc-shaped particles); σ_0 is the surface tension of the dense phase; δ serves as the Tolman parameter [44], which is the curvature correction to the surface tension (this parameter was calculated in [43]); and $O(1/R^2)$ stands for the higher order terms of the perturbation series. It was proved [43] that it is unnecessary to further refine the relationship between the surface tension and the nanoparticle radius, because the equation used to establish this relationship is valid only within the first order of $1/R$. The change in the surface tension due to the curvature of the nanoparticles is sufficiently large to exert an appreciable effect on the nucleation process [45].

ACKNOWLEDGMENTS

This work was supported by the Russian Foundation for Basic Research (grant nos. 06-03-32467 and 07-08-00542), by state contracts (NFM-1/03, NSh-2288.2003.1), and the St. Petersburg Scientific Center. We are deeply grateful to T.V. Lavrova for assistance in the preparation of this article.

REFERENCES

1. Ehrenfest, P., *Commun. Leiden Univ.*, 1933, Suppl., p. 576.
2. Lifshits, I.M., Azbel, M.Ya., and Kaganov, M.I., *Elektronnaya Teoriya Metallov* (Electronic Theory of Metals), Moscow: Nauka, 1971.
3. Landau, L.D. and Lifshitz, E.M., *Teoreticheskaya fizika* (Theoretical Physics), vol. 5: *Statisticheskaya fizika* (Statistical Physics), Moscow: Nauka, 1995, part 1, p. 606.
4. *The Collected Works of J. Willard Gibbs*, New York: Longmans, Green, and Co., 1931.
5. Volmer, M., *Kinetik der Phasenbildung*, Dresden: Steinkopf, 1939.
6. Frenkel, Ya.I., *Kineticheskaya teoriya zhidkostei* (Kinetic Theory of Liquids), Moscow: Akad. Nauk SSSR, 1945.
7. Becker, R. and Döring, W., *Ann. Phys.*, 1935, vol. 24, p. 719.
8. Zel'dovich, Ya.B., *Zh. Eksp. Teor. Fiz.*, 1942, vol. 12, no. 11/12, p. 525.
9. Kashchiev, D., *Nucleation Basic Theory with Applications*, Oxford: Butterworth Heinemann, 2000, p. 83.
10. Kuni, F.M., Shchekin, A.K., and Grinin, A.P., *Usp. Fiz. Nauk*, 2001, vol. 171, no. 4, p. 346.
11. Slezov, V.V. and Schmelzer, J.W., *Phys. Rev. E: Stat. Phys., Plasmas, Fluids, Relat. Interdiscip. Top.*, 2002, vol. 65, p. 031 506.
12. Skripov, V.P. and Faizulin, M.Z., *Fazovye perekhody zhidkost'-par i termodinamicheskoe podobie* (Liquid-Vapor Transitions and Thermodynamic Similarity), Moscow: Fizmatlit, 2003.

13. Shneidman, V.A., *Phys. Rev. A: At., Mol., Opt. Phys.*, 1991, vol. 44, p. 2609.
14. Kukushkin, S.A. and Osipov, A.V., *Prog. Surf. Sci.*, 1996, vol. 151, no. 1, p. 1.
15. Kukushkin, S.A. and Osipov, A.V., *Usp. Fiz. Nauk*, 1998, vol. 168, no. 10, p. 1083.
16. Kukushkin, S.A. and Osipov, A.V., in *Encyclopedia of Nanoscience and Nanotechnology*, Nalwa, H.S., Ed., Los Angeles: American Scientific Publishers, 2004, vol. 8, p. 113.
17. Kukushkin, S.A. and Osipov, A.V., *Phys. Rev. B: Solid State*, 2002, vol. 65, p. 174101.
18. Osipov, A.V., *Thin Solid Films*, 1993, vol. 227, p. 111.
19. Kukushkin, S.A. and Slezov, V.V., *Dispersnye sistemy na poverkhnosti tverdykh tel (evolyutsionnyi podkhod): mekhanizmy obrazovaniya tonkikh plenok* (Disperse Systems on Solid Surfaces (Evolutionary Approach): Solid Film Formation Mechanisms), St. Petersburg: Nauka, 1996.
20. Lifshits, I.M. and Slezov, V.V., *Zh. Eksp. Teor. Fiz.*, 1958, vol. 35, no. 2, p. 479.
21. Kukushkin, S.A. and Osipov, A.V., *Zh. Eksp. Teor. Fiz.*, 1998, vol. 113, no. 6, p. 2197.
22. Kuni, F.M. and Melikhov, A.A., *Teor. Mat. Fiz.*, 1990, vol. 83, no. 2, p. 274.
23. Shneidman, V.A., *Zh. Eksp. Teor. Fiz.*, 1986, vol. 91, no. 2.
24. Slezov, V.V. and Schmelzer, J., *J. Phys. Chem.*, 1994, vol. 55, p. 243.
25. Kukushkin, S.A. and Nemna, S.V., *Dokl. Akad. Nauk*, 2001, vol. 377, no. 6, p. 1 [*Dokl. Phys. Chem.* (Engl. Transl.), vol. 377, nos. 4–6, p. 117].
26. Fradkov, A.L., Guzenko, P.Yu., Kukushkin, S.A., and Osipov, A.V., *J. Phys. D: Appl. Phys.*, 1997, vol. 30, p. 2794.
27. Kol'tsova, E.M., Tret'yakov, Yu.D., Gordeev, L.S., and Vertegrel, A.A., *Nelineinaya dinamika i termodinamika neobratimykh protsessov v khimii i khimicheskoi tekhnologii* (Nonlinear Dynamics and Irreversible Thermodynamics in Chemistry and Chemical Engineering), Moscow: Khimiya, 2001.
28. Gol'man, E.K., Gol'drin, V.I., Plotkin, D.A., and Razumov, S.V., *Fiz. Tverd. Tela*, 1997, vol. 39, no. 2, p. 204.
29. Slezov, V.V. and Sagalovich, V.V., *Usp. Fiz. Nauk*, 1987, vol. 151, no. 1, p. 67.
30. Eaglesham, D.J. and Cerullo, M., *Phys. Rev. Lett.*, 1990, vol. 64, p. 1943.
31. Schukin, V.A., Bimberg, D., *Rev. Mod. Phys.*, 1999, vol. 71, p. 1125.
32. Shchukin, V.A., Ledentsov, N.N., Kop'ev, P.S., and Bimberg, D., *Phys. Rev. Lett.*, 1995, vol. 75, p. 2968.
33. Pchelyakov, O.P., Bolkhovityanov, Yu.B., Dvurechenskii, A.V., Nikiforov, A.I., Yakimov, A.I., and Voigtlander, B., *Thin Solid Films*, 2000, vol. 367, p. 75.
34. Alferov, Zh.I., *Semiconductors*, 1998, vol. 32, no. 1, p. 3.
35. Bolkhovityanov, Yu.B., Pchelyakov, O.P., and Chikichev, S.I., *Usp. Fiz. Nauk*, 2001, vol. 171, p. 689.
36. Osipov, A.V., Schmitt, F., Kukushkin, S.A., and Hess, P., *Phys. Rev. B: Solid State*, 2001, vol. 64, p. 205421.
37. Kukushkin, S.A., Osipov, A.V., and Khess, R., *Fiz. Tekh. Poluprovodn.* (St. Petersburg), 2002, vol. 36, no. 10, p. 1177 [*Semiconductors* (Engl. Transl.), vol. 36, no. 10, p. 1097].
38. Dubrovskii, V.G., Cirlin, G.E., and Ustinov, V.N., *Phys. Rev. B: Solid State*, 2003, vol. 68, p. 075409.
39. Kukushkin, S.A., *Usp. Mekh.*, 2003, vol. 2, no. 2, p. 21.
40. Kukushkin, S.A., *J. Appl. Phys.*, 2005, vol. 98, p. 033503-1.
41. Kukushkin, S.A., Osipov, A.V., and Shlyagin, M.G., *Zh. Tekh. Fiz.*, 2006, vol. 76, no. 8, p. 73 [*Tech. Phys.* (Engl. Transl.), vol. 76, no. 8, p. 1035].
42. Cheremskoi, P.G., Slezov, V.V., and Betekhtin, V.I., *Pory v tverdom tele* (Pores in Solids), Moscow: Energoatomizdat, 1990.
43. Gordon, P.V., Kukushkin, S.A., and Osipov, A.V., *Fiz. Tverd. Tela*, 2002, vol. 44, no. 11, p. 2079.
44. Tolman, R.C., *J. Chem. Phys.*, 1949, vol. 17, p. 333.
45. Brodskaya, E.N., Eriksson, J.C., Laaksonen, A., and Rusanov, A.I., *J. Colloid Interface Sci.*, 1996, vol. 180, no. 1, p. 86.